PHYSICAL REVIEW B **81**, 020301(R) (2010)

Ballistic heat transport in nanocontacts

T. Y. Chen and C. L. Chien
Department of Physics and Astronomy, The Johns Hopkins University, Baltimore, Maryland 21218, USA

M. Manno, L. Wang,* and C. Leighton
Department of Chemical Engineering and Materials Science, University of Minnesota, Minneapolis, Minnesota 55455, USA

(Received 25 November 2009; published 7 January 2010)

We have determined the ballistic heat transport relation of $V^2=C(T_m-T)$ in nanocontacts involving the bias voltage V, the ambient temperature T, and the maximum temperature T_m inside the contact by exploiting the ordering temperature of a magnetic solid as a natural thermometer. The relation has been further established using a single contact at one temperature but different magnetic fields. A simple energy-transfer model incorporating ballistic transport can qualitatively account for this relation. We also demonstrate a ballistic transport method for determining the ordering temperatures of magnets.

DOI: 10.1103/PhysRevB.81.020301 PACS number(s): 72.15.Eb, 73.23.Ad, 73.40.Jn, 74.50.+r

Joule heat generation in electrical contacts is inevitable and thermal management is essential for all electronic devices. Indeed, heat dissipation, and not circuitry, has already limited the clock speed of microprocessors.[1] The characteristics of Joule heat are fundamentally different for diffusive and ballistic transport, in which the structural length scale is, respectively, larger or smaller than that of the carrier mean free path l.[2–9] Since l is less than 100 nm for most materials, most electronic devices to date operate in the diffusive limit, for which the behavior of diffusive heat transport is well known. In contrast, ballistic heat transport, which will prevail in nanoscale ballistic charge- and spin-based devices, remains poorly understood theoretically or experimentally. In fact, the experimental framework for the investigation of such effects does not yet exist. This is due to two primary difficulties: the nanoscale dimensions of the device and the lack of suitable method to measure the local temperature rise within a ballistic contact.

Diffusive and ballistic transport can be addressed through a circular constriction of radius a. The transport is in the diffusive (Maxwell) limit or the ballistic (Sharvin) limit when a is, respectively, much larger or smaller than l. The Maxwell and Sharvin resistances of the constriction are, respectively, $\rho/2a$ and $4\rho l/3\pi a^2$,[10] where ρ is the resistivity. When an electrical voltage V is applied to the contact, the temperature within the contact rises due to Joule heating. For diffusive point contacts, the relation has been well established as[11]

$$V^2 = 4L(T_m^2 - T^2), \tag{1}$$

where T is the ambient temperature, T_m is the maximum temperature inside the contact, and L is the Lorentz constant. This relation can be theoretically deduced assuming that thermal and electrical currents coincide and that the Wiedemann-Franz law holds.

The exploration of ballistic charge or spin transport in recent years led to the discovery of giant magnetoresistance and spin transport torque (STT) effects using nanopillars and point-contact spectroscopy (PCS).[12–14] The study of phonon and magnon excitations using ballistic transport and PCS was reported even earlier.[15,16] Conspicuously lacking is ballistic heat transport, which remains poorly understood despite its importance. Some have suggested that ballistic transport would generate little Joule heat except those transmitted from adjacent regions due to diffusive scattering.[4–7] Others have proposed that ballistic heat can be generated within the contact by oscillating defects[17,18] and atoms.[2,3] Regardless of the basic mechanisms, there are ample indications[17–20] that the characteristics of ballistic heat transport are quite different from those of diffusive heat transport. For example, heat transport through larger Al/Al point contacts can be well described by Eq. (1), but not those in much smaller contacts.[21] Without the ballistic heat transport relation, some have used Eq. (1) for diffusive heat transport to address ballistic heat transport in nanodevices.[22,23] The main challenge in addressing ballistic heat transport experimentally is the determination of the temperature inside the nanocontacts.

In this work, we have quantitatively established the ballistic heat transport relationship in ballistic contacts by exploiting the magnetic ordering temperature as an imbedded thermometer. At a given ambient temperature, a nanoregion underneath the point contact can be heated to its magnetic ordering temperature by a unique bias voltage V_C, whose value is uniquely defined and independent of the contact resistance. The ballistic heat transport relation has been further established by using one contact at a fixed temperature but different magnetic fields. A simple heat transfer model can account for the ballistic transport relation. The ballistic heat transport relation also allows a method for measuring the ordering temperature of a magnetic solid.

The Curie temperature T_C of a ferromagnet or the Néel temperature T_N of an antiferromagnet marks a magnetic phase transition, which can be revealed by magnetometry and electrical resistivity measurements. In the case of a single-crystal ferromagnetic CoS_2 (Ref. 24) with a high residual resistivity ratio $RRR=\rho(300\ K)/\rho(5\ K)=160$, the temperature dependence of magnetization $M(T)$ and $dM(T)/dT$ at various magnetic fields H as measured by a superconducting quantum interference device magnetometer are shown in Figs. 1(a) and 1(b), respectively. At $H=0.01$ T, $M(T)$ shows a sharp transition with a sharp dip in $dM(T)/dT$ at $T_C \approx 120$ K. With increasing H, the transition in $M(T)$ and the dip in $dM(T)/dT$ broaden and shift to higher temperatures as expected.[25,26] The resistance $R(T)$ and $dR(T)/dT$ show similar behaviors as shown in Figs. 1(c) and

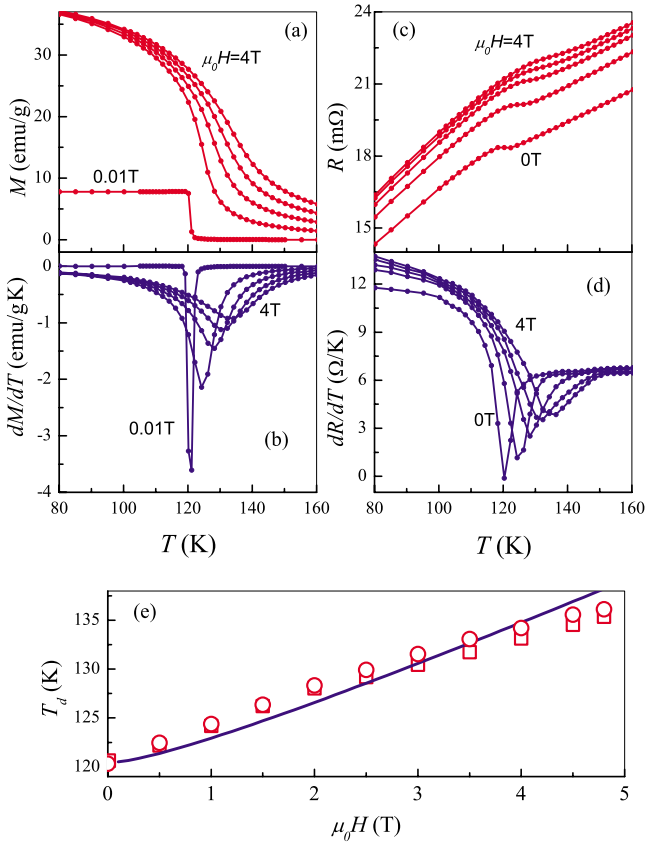

FIG. 1. (Color online) Temperature dependence of (a) magnetization $M(T)$, (b) dM/dT, (c) resistance $R(T)$, and (d) dR/dT of single crystal CoS_2 in various fields (μ_0H=0.01, 1, 2, 3, and 4 T). (e) The dip temperature T_d from (b) and (d) as a function of H (solid line is from mean-field calculation).

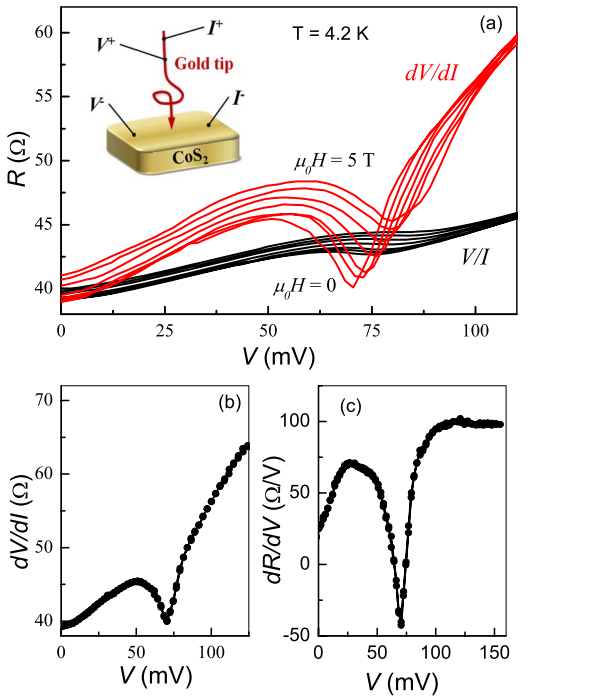

FIG. 2. (Color online) (a) Resistance V/I and differential resistance dV/dI of an Au/CoS_2 point contact as functions of the bias voltage and the schematics of the experimental setup (inset) at μ_0H=0, 0.5, 1, 2, 3, 4, and 5 T, and the comparison at zero field of (b) dV/dI and (c) $dR(V)/dV$ calculated from $(1-RdI/dV)/I$.

1(d), respectively. The dip temperatures T_d in dM/dT and dR/dT are essentially the same, increasing with H, and can be described by a simple mean-field theory [solid curve in Fig. 1(e)]. We exploit the sharp feature in $R(T)$ at the ordering temperature of a magnetic solid as an imbedded thermometer.

The point-contact setup of a gold (Au) tip on CoS_2 single crystal is schematically shown in the inset of Fig. 2(a). In ballistic transport the contact resistance is the Sharvin resistance of $R_{PC}=4\rho l/3\pi a^2$. Since $\rho l \approx 10^{-15}$ m^2 Ω for common metals, R_{PC} is in the range of 1–100 Ω for contact size a between 1.8 and 18 nm. With l about 120 nm determined from $\rho \approx 0.86$ μΩ cm for CoS_2 and 0.79 μΩ cm for the gold tip at 4.2 K, all the contacts are ballistic in nature. A representative ballistic transport result of CoS_2 at 4.2 K with $R_{PC}(V \approx 0)=39.4$ Ω at $H=0$ is shown in Fig. 2(a), where the resistance (V/I) exhibits minima at ±70.43 mV, revealed as sharp dips in the simultaneously measured differential resistance (dV/dI). The feature is nonhysteretic and appears symmetrically on both polarities of voltage. The dip shifts progressively to higher V value and becomes broader in magnetic fields, as shown in Fig. 2(a). The conductance results at 4.2 K of various Au/CoS_2 contacts are shown in Fig. 3(a). Remarkably, for *all* the different Au/CoS_2 contacts measured at different times each with a different value of R_{PC}, the resistive transition occurs at the *same* voltage of V_C=70.43 mV. Furthermore, the critical power $P_C=V_CI_C$ varies linearly with R_C^{-1} with $R_C \equiv V_C/I_C$, as shown in Fig. 3(c).

The value of V_C, uniquely defined at each temperature, independent of contact resistance, decreases with temperature and vanishes at T_C as shown in Figs. 4(a)–4(c). The nonhysteretic symmetric features appearing for both polarities of voltage are not due to the STT effect or magnon excitations, which is distinctively asymmetrical and occurring for only one polarity of voltage.[12–14] The features are not due to phonon excitations either since they are strongly affected by the external magnetic field as shown in Fig. 2(a). The unique value of V_C for all the contacts might suggest a feature related to the density of states at the Fermi level. This possibility can be ruled out because the measured V_C increases with the applied magnetic field and decreases with temperature. Instead, the field dependence of V_C and the fact that V_C vanishes right at T_C indicate that the feature at V_C is intimately associated with the magnetic transition at T_C at which the resistivity displays a transition as shown in Figs. 1(c) and 1(d). Indeed, the step in V/I and the dip in dV/dI mark the resistive transition at T_C of the nanoregion underneath the point contact due to ballistic heating. Specifically, at V=70.43 mV and R_{PC}=39.4 Ω, a current of 1.79 mA with a current density of 7.0×10^9 A/cm^2 has ballistically heated the nanoregion from 4.2 K to T_C=120 K. This conclusion can be further strengthened by the comparison between $dR(T)/dT$ in Fig. 1(d) and $dR(V)/dV$, which can be calculated from the measured dV/dI as $(1-RdI/dV)/I$. The results of $dR(V)/dV$ [Fig. 2(c)] showing a similar dip as

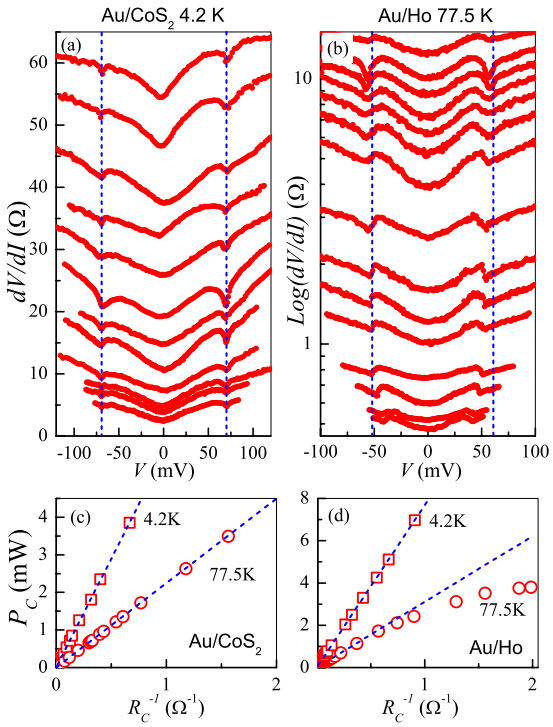

FIG. 3. (Color online) Differential resistance dV/dI curves of representative contacts with various contact resistances as functions of bias voltage with dips at $\pm V_C$ shown by the dashed lines: (a) for Au/CoS_2 contacts at 4.2 K, (b) for Au/Ho contacts at 77.5 K on logarithmic scale, (c) critical power ($P_C=I_CV_C$) as a function of R_C^{-1} for Au/CoS_2 contacts at 4.2 and 77.5 K, and (d) for Au/Ho contacts at 77.5 K The dashed lines in (c) and (d) are linear fits for R_C^{-1} less than 1 Ω^{-1}.

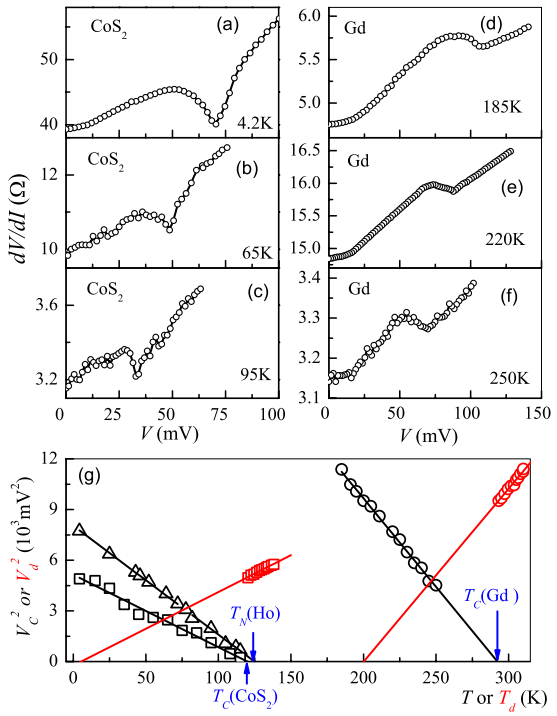

FIG. 4. (Color online) Representative dV/dI curves of (a)–(c) Au/CoS_2 contacts and (d)–(f) Au/Gd contacts at various temperatures, and (g) V_C^2 as a function of the temperature T for Au/Ho contacts (open triangles), Au/CoS_2 contacts (open squares), and Au/Gd contacts (open circles). The solid lines are results of linear fit. Red squares and circles on lines with positive slopes are V_d^2 as a function of the dip temperature T_d obtained from dR/dT in the same field for CoS_2 and Gd, respectively, with red lines (sloping upward) as the best fit results. The values of T_N and T_C in bulk Ho, CoS_2, and Gd are indicted by the vertical blue arrows.

dR/dT [Fig. 1(d)] conclusively demonstrated ballistic heating.

The value of V_C of CoS_2 at all temperatures can be described by a single relation of $V_C^2=42.9(119.7-T)=C(T_C-T)$ as shown in Fig. 4(g) by the open squares. We have in fact experimentally determined the ballistic heat transport relation of

$$V^2 = C(T_m - T), \tag{2}$$

where T_m is the maximum temperature within the contact, T is the ambient temperature, and C is a material specific parameter. The significance of this relation will be discussed later.

We describe a simple model to qualitatively account for the observed ballistic heating relation. For simplicity, we assume a cylindrical nanoregion of height h and a basal area $S=\pi a^2$, defined by the contact size $2a$ in the range of 3.6–36 nm. When a voltage V is applied to a nanoregion, its temperature rises to a steady-state temperature T_m, at which the electrical power $P=V^2/R_{PC}$ is balanced by the heat conduction $S\kappa\nabla T$ via an effective thermal conductivity κ. In ballistic contacts, $R_{PC}=4\rho l/3\pi a^2=4\rho l/3S$; hence, $V^2 \approx 4\rho l\kappa\nabla T/3$. We take a linear approximation for the gradient ∇T as $2(T_m-T)/h$ between the contact at T_m and outside at T. The height h is related to the inelastic mean free path and is expected to be proportional to κ. Since $\rho l \approx$ const and $\kappa \propto h$, $V^2 \propto (T_m-T)$, which is the key result of ballistic heating. This simple model can also qualitatively account for the diffusive heat transport relation by using the Maxwell resistance $R_{PC}=\rho/2a$ in $V^2/R_C=S\kappa\nabla T$, resulting in $V^2=\pi a\rho\kappa(T_m-T)/h$. Because of the coincidence of electric and thermal currents ($h \approx a$) and that the Wiedemann-Franz law be approximated as $\rho\kappa=L(T_m+T)/2$, one has the diffusive heating relation of $V^2 \propto L(T_m^2-T^2)$.

In addition to CoS_2, we have also observed the ballistic transport behavior in ferromagnetic Gd ($T_C=294$ K) with representative results in Figs. 4(d)–4(f) and antiferromagnetic Ho ($T_N=124$ K) with representative results in Fig. 3(b). The value of V_C, again uniquely defined for each ambient temperature and independent of the contact resistance R_C, decreases with increasing T. The linear relation $V_C^2=104.64(294.30-T)$, shown in Fig. 4(g) (as open circles), accurately determines $T_C=294.30$ K. The method is also applicable for antiferromagnetic Ho, for which we have obtained $V_C^2=64.33(124.84-T)$, yielding correctly $T_N=124.84$ K as shown in Fig. 4(g) (open triangles). We have in fact demonstrated a method for measuring the ordering temperature of either a ferromagnet or an antiferromagnet by ballistic heating a nanoregion while maintaining specimen at a low temperature. This rapid method[7] administered to a nanoregion is insensitive to the inevitable inhomogeneity in bulk specimens. It paves the way for scanning probe implementation to map the local ordering temperature with nanometer lateral resolution.

The ballistic or diffusive nature can be controlled by varying the contact size. In the case of polycrystalline Ho, ballistic contacts have been achieved at 4.2 K with R_{CP} above 1 Ω and P_C depends linearly on R_C^{-1} as shown in Fig. 3(d), but not at 77.5 K, where contacts with R_C^{-1} larger than about 1 Ω^{-1} are increasingly more diffusive because of the increasing size of the contact. Hence, the value of P_C deviates from the linear relationship at large values of R_C^{-1} as shown in Fig. 3(d), distinctively demonstrating the different characteristics between ballistic and diffusive heat transports.

The ballistic heating relation, $V_C^2=C(T_C-T)$, established from many contacts at different temperatures, can be revealed in another way by using only one contact at one temperature but different magnetic fields. As shown in Fig. 1(d), The dip temperature T_d in $dR(T)/dT$ shown in Fig. 1(d) and the dip voltage V_d in dV/dI shown in Fig. 2(a) in the ballistic measurements of Au/CoS_2 at 4.2 K both shift to higher temperature with increasing H. Similar behavior has also been observed in Au/Gd contacts maintained at the same ambient temperature of 200 K. The values of V_d^2 in both cases are linear in T_d as shown by the lines with positive slopes of $V_d^2=43.51(T_d-5.28)$ and $V_d^2=102.39(T_d-200.13)$ for the Au/CoS_2 contacts at 4.2 K (red squares) and the Au/Gd contacts at 200 K (red circles), respectively, in Fig. 4(g). For the Au/CoS_2 contacts, V_d vanishes at 5.28 K—close to the actual temperature of 4.2 K—and for the Au/Gd contacts V_d vanishes at 200.13 K, again close to the actual temperature of 200 K. Furthermore, the prefactors of 43.51 and 102.39 are very close to the values of 42.90 and 104.64 obtained earlier by varying only the temperature. These results further show that the ballistic heating relation $V^2=C(T_m-T)$ is generally valid and that C is a material specific constant independent of both T and H.

The relation $V^2=C(T_m-T)$ that we have determined for ballistic contacts is very different from $V^2=4L(T_m^2-T^2)$ for diffusive transport. Using $C=50$ $(mV)^2/K$ and $L=0.0245$ $(mV)^2/K^2$, these two relations have a crossover point at about 500 K, below which the heat generation is much less in ballistic contacts, a very important advantage for nanodevices. We can also estimate the value of C, which in our simple model is approximately $8\rho l\kappa/3h$. Using $\rho l \approx 1$ Ω fm for most metals, we take $\kappa=21$ W/cm K for Au at 4 K, and $h\approx 100$ nm, the mean free path at 4 K, we obtain $C\approx 56$ mV^2/K, which is in very good agreement with the measured values ranging from 43 to 103 mV^2/K. Our simple model, which is based on energy conservation, diffusive Joule heat, a linear approximation of the temperature gradient, and the Fourier's law with diffusive thermal conductivity, can qualitatively account for our experimental results, while a quantitative model awaits theoretical implementation.

In conclusion, we have determined the ballistic heating relation of $V^2=C(T_m-T)$, in which the square of voltage depends linearly on the difference between the maximum temperature inside the contact and the ambient temperature. This relation is valid with or without a magnetic field. A simple energy-transfer model with ballistic properties of the point contact can account for this relationship. We show that the ordering temperatures of magnetic solids can be determined by ballistic transport at temperatures far below the actual ordering temperature.

Works at Johns Hopkins University and at the University of Minnesota were supported by the NSF MRSEC program.

*Present address: School of Physical and Mathematical Science, Nanyang Technological University, Singapore.

[1] K. Banerjee and A. Merhotra, IEEE Circuits Devices Mag. **17**, 16 (2001).
[2] T. N. Todorov, Philos. Mag. B **77**, 965 (1998).
[3] M. J. Montgomery and T. N. Todorov, J. Phys.: Condens. Matter **15**, 8781 (2003).
[4] M. Rokni and Y. Levinson, Phys. Rev. B **52**, 1882 (1995).
[5] V. L. Gurevich, Phys. Rev. B **55**, 4522 (1997).
[6] V. L. Gurevich and M. I. Muradov, J. Phys.: Condens. Matter **18**, 11217 (2006).
[7] Y. C. Chen, M. Zwolak, and M. D. Ventra, Nano Lett. **3**, 1691 (2003).
[8] D. G. Cahill, W. K. Ford, K. E. Goodson, G. D. Mahan, A. Majumdar, H. J. Maris, R. Merlin, and S. R. Phillpot, J. Appl. Phys. **93**, 793 (2003).
[9] G. Chen, Phys. Rev. Lett. **86**, 2297 (2001).
[10] Yu. V. Sharvin, Zh. Eksp. Teor. Fiz. **48**, 984 (1965) [Sov. Phys. JETP **21**, 655 (1965)].
[11] R. Holm, *Electric Contact*, 4th ed. (Springer, New York, 1967), Sec. 13.
[12] M. Tsoi, A. G. M. Jansen, J. Bass, W.-C. Chiang, M. Seck, V. Tsoi, and P. Wyder, Phys. Rev. Lett. **80**, 4281 (1998).
[13] E. B. Myers, D. C. Ralph, J. A. Katine, R. N. Louie, and R. A. Buhrman, Science **285**, 867 (1999).
[14] T. Y. Chen, Y. Ji, C. L. Chien, and M. D. Stiles, Phys. Rev. Lett. **93**, 026601 (2004).
[15] A. M. Duif, A. G. M. Jansen, and P. Wyder, J. Phys.: Condens. Matter **1**, 3157 (1989).
[16] I. K. Yanson, Zh. Eksp. Teor. Fiz. **66**, 1035 (1974) [Sov. Phys. JETP **39**, 506 (1974)].
[17] K. S. Ralls and R. A. Buhrman, Phys. Rev. Lett. **60**, 2434 (1988).
[18] P. A. M. Holweg, J. Caro, A. H. Verbruggen, and S. Radelaar, Phys. Rev. B **45**, 9311 (1992).
[19] C. J. Muller, J. M. van Ruitenbeek, and L. J. de Jongh, Phys. Rev. Lett. **69**, 140 (1992).
[20] J. M. Krans, J. M. van Ruitenbeek, V. V. Fisun, I. K. Yanson, and L. J. de Jongh, Nature (London) **375**, 767 (1995).
[21] R. S. Timsit, IEEE Trans. Compon. Packag. Technol. **29**, 727 (2006).
[22] D. Fuchs, I. N. Krivorotov, P. M. Braganca, N. C. Emley, A. G. F. Garcia, D. C. Ralph, and R. A. Buhrman, Appl. Phys. Lett. **86**, 152509 (2005).
[23] A. G. M. Jansen, A. P. van Gelder, and P. Wyder, J. Phys. C **13**, 6073 (1980).
[24] L. Wang, T. Y. Chen, C. L. Chien, and C. Leighton, Appl. Phys. Lett. **88**, 232509 (2006).
[25] L. Wang, T. Y. Chen, and C. Leighton, Phys. Rev. B **69**, 094412 (2004).
[26] I. A. Campbell and A. Fert, *Ferromagnetic Materials* (North-Holland, Amsterdam, 1982), Vol. 3, p. 747.